Collision of propagating vortices embedded within Airy beams

2013 J. Opt. 15 044001

(http://iopscience.iop.org/2040-8986/15/4/044001)

IOP Publishing Journal of Optics
J. Opt. **15** (2013) 044001 (6pp) doi:10.1088/2040-8978/15/4/044001

Collision of propagating vortices embedded within Airy beams

C Rosales-Guzmán[1], M Mazilu[2], J Baumgartl[2], V Rodríguez-Fajardo[1], R Ramos-García[1] and K Dholakia[2]

[1] Instituto Nacional de Astrofísica, Óptica y Electrónica, A. P. 51 y 216, 72000 Puebla, Puebla, Mexico
[2] SUPA, School of Physics and Astronomy, University of St Andrews, North Haugh, St Andrews, UK

E-mail: michael.mazilu@st-andrews.ac.uk

Received 1 November 2012, accepted for publication 24 January 2013
Published 10 April 2013
Online at stacks.iop.org/JOpt/15/044001

Abstract
We present the engineered collision of two curvilinear propagating optical vortices each embedded in the main lobe of an Airy beam. Two cases are analyzed: the same and opposite unitary topological vortex charge. We observed experimentally that in the first case the main vortices repel each other and remain separated after the collision. In contrast, in the second case an annihilation of the main vortices occurs. Our experimental observations are reinforced by numerical simulations showing that the conservation of topological charge dictates the vortex dynamics.

Keywords: optical vortices, Airy beams

S Online supplementary data available from stacks.iop.org/JOpt/15/044001/mmedia

(Some figures may appear in colour only in the online journal)

1. Introduction

Phase singularities are established as generic features of wave physics and denote regions of zero wave intensity where the phase is not defined. Their generation and evolution dictates the dynamics of many physical phenomena. In the domain of optics, following the seminal paper by Nye and Berry [1], the field of singular optics is devoted to this topic and continues to attract considerable attention. Optical beams with phase singularities are characterized by intensity zeros (due to destructive interference) where the phase is undetermined. The phase circulation around such points defines a vortex which is typically quantized in multiples of $2\pi q$, where q is the topological charge of the vortex. Optical vortices can be observed in the interference of three or more waves [2, 3] as well as in a speckle pattern [4]. The most common vortex beams possess topological charges attributed to the helicoidal spatial structure of the wavefront. Beams possessing such topological charges are often referred to as vortex beams. Phase singularities can also be seen as topological objects embedded in wavefront surfaces, possessing topological charges that behave very much like charged particles [5]. Topological interactions of vortices can lead to the creation, annihilation or even nucleation of vortices in various systems. As an example, interesting effects such as attraction followed by annihilation of a pair of vortices with opposite topological charge, or repulsion after creation of a pair of vortices with identical topological charge have been reported widely in the literature [6–11]. Intriguingly, vortices can be embedded in propagation invariant light beams, such as Mathieu and Bessel beams [12], where they typically propagate in straight lines.

The Airy beam was first discovered in quantum mechanical systems [13]. In this context, the Airy wavepacket describes a rather surprising dispersion-free solution to the Schrödinger equation, where the particle exhibits a constant transverse acceleration. Using the paraxial approximation it is straightforward to transfer this solution into an optical field [14] and show its fundamental properties [15], making an important link between quantum mechanics and paraxial wave optics. An Airy beam may also have a phase singularity embedded into its main lobe, also known as a vortex Airy (VoAi) beam [16]. Such a vortex experiences, within a certain range, the same transverse quadratic acceleration as the Airy beam. More importantly, different topologically charged VoAi beams form an orthogonal base similar to

the Laguerre–Gaussian beams, replacing the Gaussian carrier beam by an Airy beam. This allows, via superpositions, the construction of more complex beams that are also laterally accelerating. A subsequent study has explored the propagation dynamics of a single vortex in such a case [17]. However, to date the evolution and interaction of vortices embedded in Airy beams has never been explored.

In this paper, we report the first experimental observation of the controlled interaction and collision of two vortex Airy beams. Both are generated simultaneously in the same transverse plane, each with an opposite inwards transverse acceleration. Initially, a separation between the vortices exists, but as the VoAi beams propagate, they are forced to collide. We report the collision for two specific cases: identical ($q = +1$) and opposite ($q = \pm 1$) topological charges. In the former, a repulsion of vortices was observed, contrary to the second case, where an annihilation of vortices occurred. Our experimental observations are supported by theoretical simulations performed using analytical expressions for the VoAi.

2. Airy-vortex beams

The approach we used to derive an analytical expression of the VoAi beam comprises the use of an Airy phase mask endowed with a phase singularity, implemented using a spatial light modulator (SLM). This is illuminated by a Gaussian beam. We consider the VoAi to be created in the Fourier plane of a lens positioned at a distance equal to the focal length f away from the phase mask. Within the paraxial approximation, the plane defined by the phase mask corresponds to the Fourier transform of the VoAi field. In this plane, the field profile is given by

$$\begin{aligned} &u(k_x, k_y, z_0) \\ &= (k_x + \mathrm{i}k_y)^q \exp\left(-a_0 x_0^2 \left[k_x^2 + k_y^2\right]\right) \\ &\quad \times \exp\left(\frac{\mathrm{i}}{3}[x_0^3(k_x^3 + k_y^3) - 3a_0^2 x_0(k_x + k_y) - 2\mathrm{i}a_0^3]\right), \end{aligned} \quad (1)$$

with x_0 and a_0 the two characteristic parameters of the Airy beam, and k_x and k_y the Cartesian position coordinates in the SLM plane. The first term corresponds to the phase singularity, responsible for the creation of the vortex of order q. The second term is the incident Gaussian beam. And the third term is the cubic phase that generates the Airy beam.

The VoAi will be reconstructed at a distance f away from the lens. In order to reconstruct the field $u(x, y, z)$ we need to propagate the beam through a paraxial optical system defined by the general ABCD matrix. Hence, by taking into account the propagation from the phase mask to the lens ($\mathbb{P}_1$), the transmission through the same ($\mathbb{T}$) and the propagation after the lens ($\mathbb{P}_2$), we obtain

$$\begin{pmatrix} A & B \\ C & D \end{pmatrix} = \mathbb{P}_2 \cdot \mathbb{T} \cdot \mathbb{P}_1 = \begin{pmatrix} \frac{-z}{f} & f \\ \frac{-1}{f} & 0 \end{pmatrix}. \quad (2)$$

The total propagation through a paraxial optical system, defined by its ABCD matrix, can be described by the generalized Huygens–Fresnel [18] integral, which will give us the analytical expression for the VoAi beam

$$u(\mathbf{r}) = \alpha \exp\left(-\mathrm{i}\frac{kD}{2B}\rho^2\right) \sum_{n=0}^{q} \frac{(\mathrm{i})^{q-n} q!}{n!(q-n)!} P_{n(q-n)}, \quad (3)$$

where $\alpha = \frac{ik}{2\pi B} \exp(\frac{2a_0^3}{3})$, $\rho^2 = x^2 + y^2$ and k is the wavevector. Coefficients P_{ij} can be obtained from the recurrence relations:

$$P_{ij} = \frac{\partial P_{(i-1)j}}{\partial c_x}, \qquad P_{ij} = \frac{\partial P_{i(j-1)}}{\partial c_y} \quad (4)$$

with the first term P_{00} defined by

$$\begin{aligned} P_{00} = \frac{4\pi^2}{a_x a_y} &\exp\left(-\frac{2b_x^3}{3a_x^6} - \frac{\mathrm{i}b_x c_x}{a_x^3} - \frac{2b_y^3}{3a_y^6} - \frac{\mathrm{i}b_y c_y}{a_y^3}\right) \\ &\times \mathrm{Ai}\left(\frac{b_x^2 - \mathrm{i}a_x^3 c_x}{a_x^4}\right) \mathrm{Ai}\left(\frac{b_y^2 - \mathrm{i}a_y^3 c_y}{a_y^4}\right) \end{aligned} \quad (5)$$

where $\mathrm{Ai}(x)$ is the Airy function. The coefficients in this expression are given by

$$\begin{aligned} a_x &= a_y = x_0, & b_x &= b_y = -a_0 x_0^2 - \mathrm{i}\frac{kA}{2B} \\ c_x &= -\mathrm{i}a_0^2 x_0 - \mathrm{i}\frac{kx}{B}, & c_y &= -\mathrm{i}a_0^2 x_0 - \mathrm{i}\frac{ky}{B}. \end{aligned} \quad (6)$$

These expressions describe the propagation of an Airy beam of arbitrary vortex order through any paraxial optical system.

3. Experimental details

3.1. Phase reconstruction method

Since the information of the location of the vortex is contained in the beam's phase, it is necessary to reconstruct its phasefront. This was performed by an *in situ* interferometric technique [19, 20]. This technique enables us to reconstruct the electric field, amplitude and phase, of the VoAi beam simultaneously. Other methods have recently been proposed for the accurate detection of optical vortices using a Shack–Hartmann wavefront sensor [21]. The method we employed for the reconstruction is the lock-in amplifier technique applied to the optical domain, in which the field of interest $E_u = A_u \exp(\mathrm{i}\phi_u)$ is interfered with a reference field $E_R = A_R \exp(\mathrm{i}\phi_R)$, where A_u, A_R, ϕ_u and ϕ_R are the amplitude and phase of each field respectively. In addition, a time varying global phase $\phi_t = \psi t$ is added to the beam of interest, ψ being a constant. As a result of the interference, the photodetector will detect a total intensity

$$I(t) \propto |A_u \exp[\mathrm{i}(\phi_u + \psi t)] + A_R \exp(\mathrm{i}\phi_R)|, \quad (7)$$

whose temporal Fourier transform is

$$\begin{aligned} \mathscr{F}\{I\} &= \int_0^T I(\tau) \exp(-\mathrm{i}\psi\tau)\, \mathrm{d}\tau \\ &\propto A_u A_R \exp[\mathrm{i}(\phi_u - \phi_R)] = E_u E_R^*. \end{aligned} \quad (8)$$

In the experiment T is chosen in such a way the temporal phase $\phi = 2\pi/T$ is an integer multiple of 2π. The attractiveness of this technique relies on the fact that computation of the Fourier transform depends only on the product of E_u and E_R. Therefore, E_u can be determined provided we have previous knowledge of E_R. For this, A_R can be computed by taking the square root of a recorded intensity image of the reference beam (for simplicity we used a Gaussian beam), i.e., $A_R \propto \sqrt{I_R}$. The estimation of ϕ_R is performed with knowledge of the gradient $\nabla\phi_R = (\partial_x\phi_R, \partial_y\phi_R)$. Each component is computed using an approximation technique based on the numerical standard 5-point stencil method of the first derivative of a function $f(x)$. In practice this method can be realized by splitting the reference beam into two beams using SLM random encoding [22]. One beam is deflected in the detector plane by a distance h in both the x- and the y-direction. According to equation (8) the Fourier transform of the total intensity detected by the CCD camera is

$$\mathcal{I}_{\alpha\beta} = \mathscr{F}\{I_{\alpha\beta}\} = E_R(x + \alpha h, y + \beta h)E_R^*(x, y) \qquad (9)$$

with $\alpha, \beta = -2, -1, 0, 1, 2$. Explicitly the phase gradient of the reference beam is

$$\nabla\phi_R = \frac{1}{12h\mathcal{I}_{00}}\begin{pmatrix}\mathcal{I}_{-20} - 8\mathcal{I}_{-10} + 8\mathcal{I}_{10} - \mathcal{I}_{20}\\ \mathcal{I}_{0-2} - 8\mathcal{I}_{0-1} + 8\mathcal{I}_{01} - \mathcal{I}_{02}\end{pmatrix}. \qquad (10)$$

To obtain the phase profile $\phi_R(x, y)$ at the detector plane, data in the above equation are fitted to the gradient of a polynomial of order n (typically $n = 6$). The phase ϕ_u can be obtained in a similar way as described above, i.e., using equation (10). Finally, the amplitude of the field of interest A_u can now be determined using equation (8).

3.2. Experimental setup

The experimental setup implemented to produce the collisions is schematically shown in figure 1. Two spatially offset co-propagating VoAi beams with opposite transverse accelerations are generated. A 10 mW He–Ne laser beam ($\lambda = 633$ nm) is expanded by a lens system L1 and L2 and directed towards a spatial light modulator (SLM, *Holoeye* with a resolution of 1920 pixels × 1080 pixels). Both VoAi beams were created simultaneously by the same SLM using random encoding [22]. The topological charge of the beams as well as their initial separation were controlled by the hologram. The collisions were observed in the far-field using the first diffracted order of the beam after reflection from the SLM. The resultant intensity pattern could be observed in real time by means of a CCD camera. This was mounted on a computer programmable servo-controlled rail, aligned along the propagation axis of the beam.

In order to track the collisions, we carried out the reconstruction of the field E_u in several parallel planes by moving the CCD camera along the rail. An example of such a field reconstruction is shown in figure 2, where a VoAi beam with $q = -1$ accelerating to the right is shown. The first row corresponds to the experimentally measured data, whereas the second row corresponds to the theoretical predictions. Both experimental and theoretical amplitudes (figures 2(a) and (d) respectively) feature the typical Airy pattern, outstanding the presence of a dark spot in their main lobes. In the phase plots (figures 2(b) and (e)) we can observe several vortices. These are easily identified by noticing that around them the phase increases monotonically from 0 (blue) to 2π (red). The handedness in which the phase increases (clockwise or counterclockwise) determines the sign of the topological charge. In order to visualize the vortices we highlighted in the phase image the phase discontinuity lines connecting pairs of oppositely charged vortices. We refer to such curves as phase-cuts and note that these curves rotate around each vortex during one optical cycle [21]. The speed and sense of rotation depends on the topological charge. Figures 2(c) and (f) show respectively experimental and theoretical plots of such phase-cuts. In these figures the main vortex, that is, the vortex in the beam's main lobe, is encircled in red. In the inner part of the beam, the vortices connected by a phase-cut do not contribute to its net charge. This is not the case in the outer part of the beam, where the lines extend to infinity. However, they do not contribute to the total charge because their charges are compensated by the corresponding vortex on the opposite border. Inevitably, in the experimentally reconstructed phase (figure 2(b)) such lines were truncated by the reconstruction method. Nevertheless, the absence of this information is not important as we are only interested in the evolution of the main vortex. The phase-cut line rising from the main vortex is neither connected to another single vortex, nor compensated by another, giving the beam its topological charge.

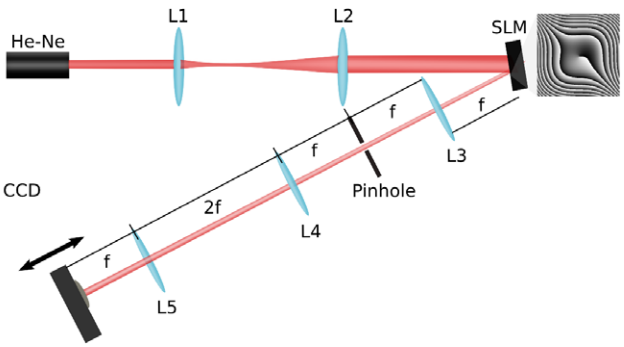

Figure 1. Schematic of the implemented experimental setup. Lens systems L1 and L2 expand the laser beam to fit the SLM screen size. Two VoAi holograms are displayed in the SLM using random encoding. The collision is tracked along the propagation axis with a CCD camera mounted in a computer-controlled railway.

4. Results

We present results showing the collision for two cases: two beams with same topological charges ($q = -1$) and two with opposite topological charges ($q = \pm 1$). Our analysis of them is restricted to the vortex embedded in the main lobe of each VoAi beam. Our experimental results are summarized in two videos (figure 3: media 1 available at

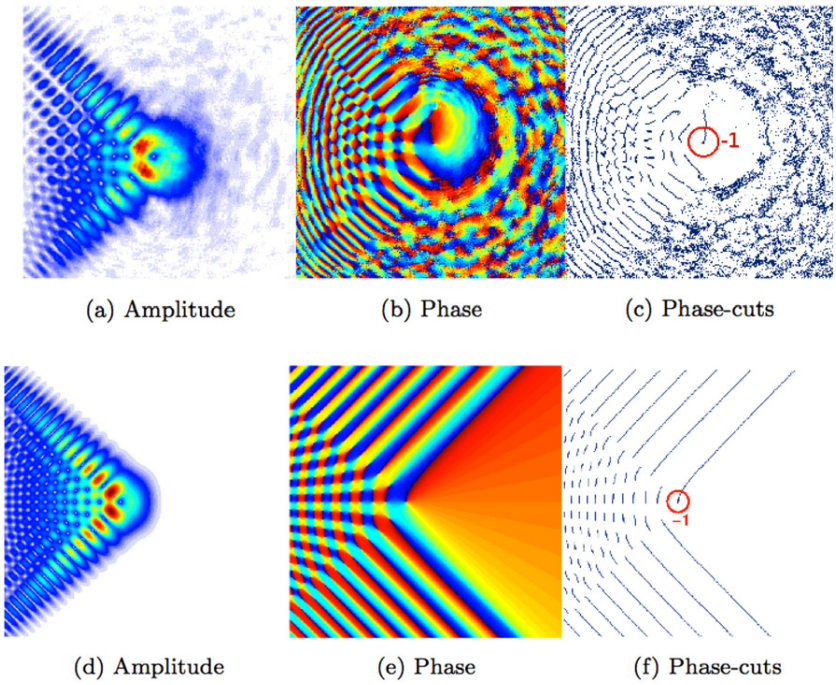

Figure 2. Experimental reconstruction (top row) and theoretical prediction (bottom row) of the electric field of a VoAi beam with topological charge $q = -1$. In (b) and (e) the phase varies from 0 (blue) to 2π (red). The phase-cuts in (c) and (f) are the discontinuity curves in the phase of (b) and (e) respectively. A vortex is found at each end(s) of a phase-cut.

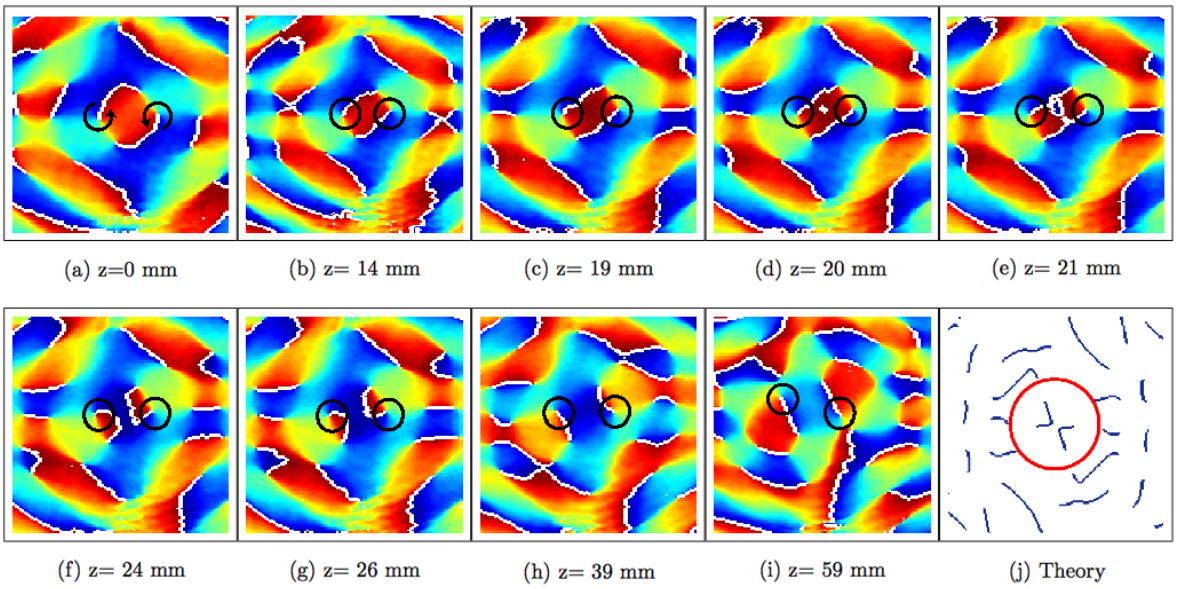

Figure 3. Collision of two VoAi beams carrying same topological charges $q = -1$ (counterclockwise). (a)–(i) Reconstructed phases of selected positions along the propagation axis. Phase-cuts are highlighted as white lines and the main vortices enclosed within black circles (in (a) their signs are represented by arrows). Media 1 (available at stacks.iop.org/JOpt/15/044001/mmedia) shows the collision in the phase-cuts domain from $z = 0$ mm to $z = 59$ mm in steps of 1 mm. (j) Image from the simulation of the collision in the phase-cuts domain (media 2 available at stacks.iop.org/JOpt/15/044001/mmedia).

stacks.iop.org/JOpt/15/044001/mmedia and figure 4: media 3 available at stacks.iop.org/JOpt/15/044001/mmedia) showing the collision in the phase-cuts domain. These are reinforced by their corresponding theoretical counterpart (figure 3(j): media 2 available at stacks.iop.org/JOpt/15/044001/mmedia and figure 4(j): media 4 available at stacks.iop.org/JOpt/15/044001/mmedia).

4.1. Equal charges

Figure 3 consists of a representative subset of images showing the collision of two equally charged VoAi beams in the phase domain. The first image corresponds to the reconstruction of the phase at the focal plane ($z = 0$ mm) and the last one at a distance of 59 mm away from it. For the sake of clarity,

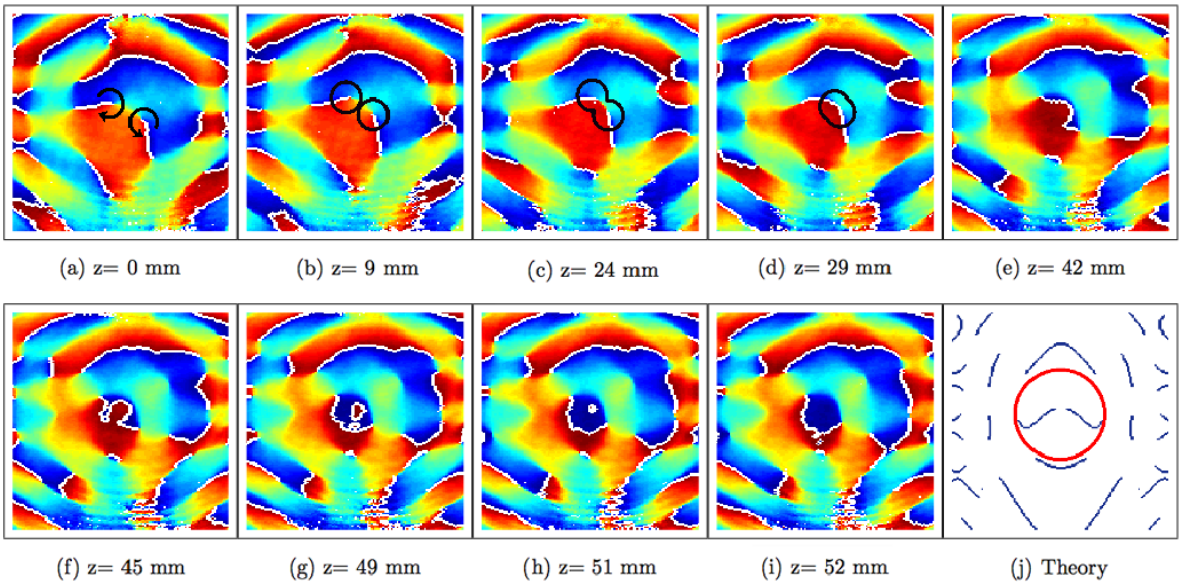

Figure 4. Collision of two VoAi beams carrying opposite topological charges $q = \pm 1$. (a)–(i) Reconstructed phases of selected positions along the propagation axis. Phase-cuts are highlighted as white lines and the main vortices enclosed within black circles (in (a) their signs are represented by arrows). Media 3 (available at stacks.iop.org/JOpt/15/044001/mmedia) shows the collision in the phase-cuts domain from $z = 0$ mm to $z = 59$ mm in steps of 1 mm. (j) Image from the simulation of the collision in the phase-cuts domain (Media 4 available at stacks.iop.org/JOpt/15/044001/mmedia).

in these images only the region where the interaction takes place is shown. Phase-cuts are emphasized as white lines and the main vortices are enclosed within black circles. In the sequence, 3(a)–(c), the main phase-cuts (the ones linked to the main vortices) bend towards each other. In frames 3(d) and (e) a change in orientation of the phase-cuts occurs, after which the phase-cuts bend away from each other (frames 3(f)–(i)). It is very important to note that during this process the vortices never approach each other despite the fact that phase-cuts indicate the Airy beams are moving towards each other. We attribute this to the fact they have the same topological charge and therefore repel each other, preventing them from coming closer. We would like to stress that neither of the two main vortices disappear during the collision. Our experimental results agree well with the theoretical predictions, as can be seen in media 2 (available at stacks.iop.org/JOpt/15/044001/mmedia) (figure 3(j)). For the sake of brevity, we do not present the case of same topological charges $q = +1$, as it behaves in the same manner.

4.2. Opposite charges

The case of opposite topological charges ($q = \pm 1$) is presented in figure 4 in an analogous way to the previous one. The first image was taken at the focal plane ($z = 0$ mm) and the last one at $z = 59$ mm. In this case, as the VoAi beams propagate accelerating towards each other, the vortices come closer (figures 4(a)–(c)). At a distance of 29 mm the main phase-cuts merge into only one (figure 4(d)), evincing the annihilation of the main vortices. After this, the remaining phase-cut line folds in, forming a closed loop (figures 4(e)–(g)). This loop shrinks as the collision goes forward until it finally disappears at a distance of 52 mm (figure 4(i)). We highlight that, contrary to the previous case, the main vortices disappear during the collision. This is not surprising since the vortices are oppositely charged. Our experimental findings are in agreement with the theoretical predictions, as can be seen in media 4 (available at stacks.iop.org/JOpt/15/044001/mmedia) (figure 4(j)).

5. Conclusion

In this work we experimentally synthesized vortex Airy beams and engineered controlled collisions between two of them. The implemented technique allowed us to induce reproducible collisions. We presented two examples: one between two VoAi beams with positive unitary charges and another with opposite charges. We emphasize the crucial role of the electric field (amplitude and phase) reconstruction method, which enables one to analyze the collisions. On one hand, for vortices of equal charges, a repulsion was observed. On the other hand, vortices of opposite charges attract each other and annihilate. This behavior is confirmed analytically as generic for VoAi and distinct from vortices embedded in Mathieu beams or the nontrivial addition of topological charges [23], for example. Our results show the conservation of topological charge in VoAi beam collisions.

Acknowledgments

We thank the UK Engineering and Physical Sciences Research Council, INAOE and CONACyT for funding. Kishan Dholakia is a Royal Society-Wolfson Merit Award holder.

References

[1] Nye J F and Berry M V 1974 Dislocations in wave trains *Proc. R. Soc.* **336** 165–90

[2] Masajada J and Dubik B 2001 Optical vortex generation by three plane wave interference *Opt. Commun.* **198** 21

[3] Padgett M J, King R P, Dennis M R and O'Holleran K 2011 Knotted and tangled threads of darkness in light beams *Contemp. Phys.* **52** 1

[4] Baranova N B, Zel'dovich B Ya, Mamaev A V, Pilipetskii N F and Shkukov V V 1981 Dislocations of the wavefront of a speckle-inhomogeneous field (theory and experiment) *JETP Lett.* **33** 195

[5] Roux F S 1993 Diffractive optical implementation of rotation transform by using phase singularities *Appl. Opt.* **32** 3715

[6] Indebetouw G 1993 Optical vortices and their propagation *J. Mod. Opt.* **40** 73–87

[7] Basistiy I V, Bazhenov V Yu, Soskin M S and Vasnetsov M V 1993 Optics of light beams with screw dislocations *Opt. Commun.* **103** 422–8

[8] Heckenberg N R, Vaupel M, Malos J T and Weiss C O 1996 Optical-vortex pair creation and annihilation and helical astigmatism of a nonplanar ring resonator *Phys. Rev.* A **54** 2369

[9] Brandão P A and Julião C S 2011 Symmetry breaking of optical vortices: birth and annihilation of singularities in the evanescent field *Opt. Lett.* **36** 1563

[10] Roux F S 1995 Dynamical behavior of optical vortices *Opt. Soc. Am.* B **12** 1215

[11] Freund I and Kessler D A 2001 Critical point trajectory bundles in singular wavefields *Opt. Commun.* **187** 71–90

[12] Durnin J 1987 Exact solutions for nondiffracting beams. I. The scalar theory *J. Opt. Soc. Am.* A **4** 651–4

[13] Berry M and Balazs N 1979 Nonspreading wave packets *Am. J. Phys.* **47** 264–467

[14] Siviloglou G A, Broky J, Dogariu A and Christodoulides D N 2007 Observation of accelerating Airy beams *Phys. Rev. Lett.* **99** 213901

[15] Baumgartl J, Mazilu M and Dholakia K 2008 Optically mediated particle clearing using Airy wavepackets *Nature Photon.* **2** 675

[16] Mazilu M, Baumgartl J, Cizmar T and Dholakia K 2009 Accelerating vortices in Airy beams *Proc. SPIE* **7430** 74300C

[17] Dai H T, Liu Y J, Luo D and Sun X W 2010 Propagation dynamics of an optical vortex imposed on an Airy beam *Opt. Lett.* **35** 4075

[18] Siegman A E 1986 *Lasers* (Mill Valley, CA: University Science Books) pp 633–5

[19] De Luca A C, Kosmeier S, Dholakia K and Mazilu M 2011 Optical eigenmode imaging *Phys. Rev.* A **84** 021803(R)

[20] Mazilu M, Baumgartl J, Kosmeier S and Dholakia K 2011 Optical eigenmodes; exploiting the quadratic nature of the energy flux and of scattering interactions *Opt. Express* **19** 933

[21] Murphy K, Burke D, Devaney N and Dainty C 2010 Experimental detection of optical vortices with a Shack–Hartmann wavefront sensor *Opt. Express* **18** 15448–60

[22] Davis J A and Cottrell D M 1994 Random mask encoding of multiplexed phase-only and binary phase-only filters *Opt. Lett.* **19** 496–8

[23] Molina-Terriza G, Recolons J and Torner L 2000 The curious arithmetic of optical vortices *Opt. Lett.* **25** 1135–7